High-Resolution Electronic Spectrum of the *p*-Difluorobenzene−Water Complex: Structure and Internal Rotation Dynamics

Cheolhwa Kang and David W. Pratt*

Department of Chemistry, University of Pittsburgh, Pittsburgh, Pennsylvania 15260

Martin Schäfer

Laboratorium für Physikalische Chemie, Eidgenössische Technische Hochschule Zürich, ETH Hönggerberg - HCI, CH-8093 Zürich, Switzerland

Received: September 4, 2004; In Final Form: November 4, 2004

The rotationally resolved $S_1 \leftarrow S_0$ electronic spectrum of the water complex of *p*-difluorobenzene (*p*DFB) has been observed in the collision-free environment of a molecular beam. Analyses of these data show that water forms a planar σ-bonded complex with *p*DFB via two points of attachment, a stronger F---H−O hydrogen bond and weaker H---O−H hydrogen bond, involving an *ortho* hydrogen atom of the ring. Despite the apparent rigidity of this structure, the water molecule also is observed to move within the complex, leading to a splitting of the spectrum into two tunneling subbands. Analyses of these data show that this motion is a combined inversion-internal rotation of the attached water, analogous to the "acceptor-switching" motion in the water dimer. The barriers to this motion are significantly different in the two electronic states owing to changes in the relative strengths of the two hydrogen bonds that hold the complex together.

Introduction

Because of the important role of water as a solvent and its ability to form hydrogen bonds with other molecules, either as a proton donor or acceptor, water-containing complexes have attracted a lot of attention in recent years, especially water complexes of aromatic molecules.[1,2] If the aromatic molecule contains a functional group with oxygen or nitrogen, it normally forms a water complex with a σ hydrogen bond. In phenol−water,[3−5] the water binds as a proton acceptor to the hydroxy group, whereas it binds as a proton donor to the oxygen of the methoxy group in anisole−water.[6−8] In aniline−water, the water acts as a proton donor to the amino group with a hydrogen bond almost perpendicular to the ring plane,[9] whereas in the nitrogen-containing heterocycles pyrrole−water[10] and indole−water,[11,12] the water forms a $N-H\text{---}OH_2$ hydrogen bond as a proton acceptor.

Other water-binding motifs exist in aromatic molecules. In the water complex of the nonpolar, hydrophobic benzene molecule, water binds with its hydrogens pointing toward the π electron system, although large amplitude motions make the elucidation of the exact structure difficult.[13−17] In complexes with more than one water molecule, the water molecules form a cluster that is hydrogen bonded to the π electron system of benzene.[6,13,18,19] In the benzene−water cation, the oxygen atom of the water molecule approaches the $C_6H_6^+$ cation in the aromatic plane, an arrangement that is about 160 cm^{-1} lower in energy than the "atop" geometry.[20]

Using IR depletion R2PI spectroscopy, Brutschy and co-workers found similar complex formation patterns for substituted benzene−water clusters.[6] According to their initial interpretation, water binds to the π electron system in 1:1 complexes with fluorobenzene or *p*-difluorobenzene (*p*DFB). However, rotational contours in REMPI spectra and ab initio calculations later showed that a planar configuration where the water forms two hydrogen bonds (F---H−O and *ortho*-H---O−H) is slightly or significantly more stable than a π bonded structure in fluorobenzene−water or *p*DFB−water, respectively.[21,22] Moreover, there are still ambiguities concerning the proper interpretation of C−F---H−O interactions. Caminati et al.[23] analyzed the F---H−O hydrogen bond in difluoromethane−water using free jet millimeter wave absorption spectroscopy. None of the observed transitions were split, suggesting that water is rigidly attached to the CH_2F_2. From the stretching force constant, it was concluded that the F---H−O interaction appears to be rather strong, almost as strong as the O−H ---O internal hydrogen bond in the water dimer.[24] The binding energy was estimated to be ∼700 cm^{-1} by assuming a Lennard-Jones potential function. However, Thalladi et al.[25] reported that the C−F group in crystalline fluorobenzenes is a very poor proton acceptor, having the characteristics of weak hydrogen bonds. Only in the absence of competing interactions is the true nature of the C−F----H−O interaction ever likely to be revealed.

Rotationally resolved electronic spectroscopy is a powerful tool for studying such phenomena because it is sensitive to both the equilibrium geometry of the complex as well as to its feasible motions. In this report, a study of the rotationally resolved UV spectrum of the complex between *p*DFB and water is presented. From analyses of the moments of inertia, the structures of the complex in its S_0 and S_1 states were determined. From analyses of splittings that appear in the spectra, motions of the attached water molecule are revealed, from which information about the relative strengths of the two hydrogen bonds that hold the complex together may be deduced.

Experimental Section

High-resolution data were obtained using the CW molecular beam laser spectrometer described in detail elsewhere.[26] *p*DFB was seeded in helium at a backing pressure of about 1 bar (monomer) or 2.7 bar (complex). For the water complex, helium

* Author to whom correspondence should be addressed. E-mail: pratt@pitt.edu.

10.1021/jp046004y CCC: $30.25
Published on Web 01/19/2005

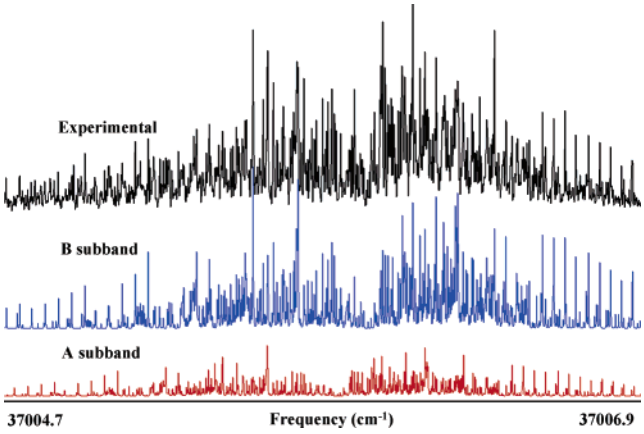

Figure 1. Rotationally resolved fluorescence excitation spectrum of the origin band of the $S_1 \leftarrow S_0$ transition of *p*DFB−H_2O, shifted 168.1 cm^{-1} to the blue of the $S_1 \leftarrow S_0$ origin band of *p*DFB. The origin band of the complex is a superposition of two subbands which are separated by 0.121 cm^{-1}. The top trace is the experimental spectrum. The second and third traces are the calculated B and A subbands, respectively.

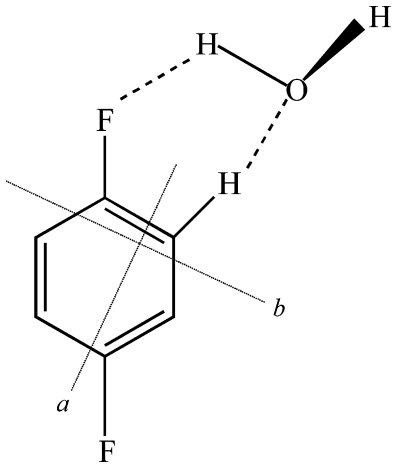

Figure 2. Approximate structure of the doubly hydrogen-bonded complex of *p*-difluorobenzene with a single water molecule. *a* and *b* denote its in-plane inertial axes.

was enriched with water vapor by passing the gas through a container holding water at room temperature. The gas mixture was expanded through a 280-μm quartz nozzle, skimmed once, and probed 15 cm downstream of the nozzle by a frequency doubled, single frequency, tunable ring dye laser operating with Rhodamine 110, yielding about 200 μW (150 μW for the monomer) of ultraviolet radiation. Fluorescence was collected using spatially selective optics, detected by a photomultiplier tube and photon-counting system, and processed by a computerized data acquisition system. Relative frequency calibrations of the spectra were performed using a near-confocal interferometer having a mode-matched FSR of 299.7520 ± 0.0005 MHz at the fundamental frequency of the dye laser. Absolute frequencies in the spectra were determined by comparison to transition frequencies in the I_2 spectrum.[27]

Results

Figure 1 shows the high-resolution spectrum of the origin band of the $S_1 \leftarrow S_0$ transition of the *p*DFB−water complex. The origin of the complex is shifted by +168.1 cm^{-1} with respect to that of the bare molecule.[28] To determine whether the spectrum contains an underlying subband structure, an autocorrelation analysis was performed to see if multiple overlapping subbands were present. This analysis revealed that there are two overlapping bands in the spectrum, separated by 3.63 GHz with significantly different relative intensities.

We initially worked to fit the stronger of these two subbands. The fitting procedure began with the simulation of a spectrum using assumed geometries of the complex. We assumed that the water lies in the plane of *p*DFB and that one O−H bond of the water is involved in the formation of a six-membered ring system with the F−C−C−H fragment of *p*DFB, as shown in Figure 2. The simulated spectrum was compared with the experimental spectrum and several transitions were assigned. An effective way to fit the spectrum is using the "selected quantum number" feature of jb95.[29] Each of the resolved lines was first assigned with $K_a = 0$ and subsequently followed by $K_a = 1, 2, 3$...because the intensity significantly decreases as K_a increases. A least-squares fit of assigned quantum numbers to the spectrum with the procedure outlined above was used to modify the assumed rotational constants. This procedure was repeated iteratively until all stronger lines were accounted for. To fit the weaker band, a second spectrum was generated using the rotational constants of the stronger subband and moved along the frequency axis on the basis of the autocorrelation results. A selected quantum number assignment was carried out in the manner described above and optimized by a least-squares fit. This fit reveals that the origin of the weaker subband is positioned at −3.63 GHz with respect to that of the stronger one, in excellent agreement with the results of the autocorrelation analysis.

A portion of the experimental spectrum, expanded to full experimental resolution from the R branch of the stronger subband, is shown in Figure 3 together with the separate calculated contributions of the two subbands in this region. Whereas the monomer exhibits a pure *b*-type spectrum,[28] the spectrum of the water complex consists of two subbands with intensity ratio 1:3 and *a*/*b* hybrid band type (about 15% *a*, 85% *b*). The rotational temperature of the complex was estimated to be about 2.5 K, and the line widths were about 30 MHz in the monomer and 40 MHz in the complex spectrum. An analysis using Voigt line shapes with a 26 MHz Gaussian component revealed Lorentzian line widths of 15 and 25 MHz for the monomer and complex, respectively, corresponding to fluorescence lifetimes of 11.5 and 6.3 ns.

Discussion

Structure of *p*DFB and Its Water Complex. Table 1 lists the inertial parameters of *p*DFB and its water complex. These data provide useful information about the structure of their ground electronic states and how these change upon electronic excitation. First, in *p*DFB itself,[28] there is a large decrease in the *A* rotational constant ($\Delta A = A' - A'' = -354.4$ MHz, −6.3%), reflecting an expansion of the ring perpendicular to the *a* inertial axis, and an increase in the *B* rotational constant ($\Delta B = 6.2$ MHz, 0.4%), suggesting a contraction of the C−C bonds adjacent to the C−F bonds. Clearly, there is enhanced conjugation of the two groups in the electronically excited state which results in a considerable decrease in the electron density on the F atoms. More quantitatively, the excited-state rotational constants can be interpreted in terms of a contraction of about 0.03 Å in the C−F bond lengths and an increase of about 2.4° in the C−C(F)−C angles.

Inertial defects (ΔI) often are used as measure of a molecule's planarity. For a rigid planar structure, ΔI is zero whereas for a rigid nonplanar structure, ΔI is negative. Concerning the *p*DFB−water complex, the magnitudes of its inertial defects are relatively small ($\Delta I'' = -0.68$ amu $Å^2$ in the ground state and

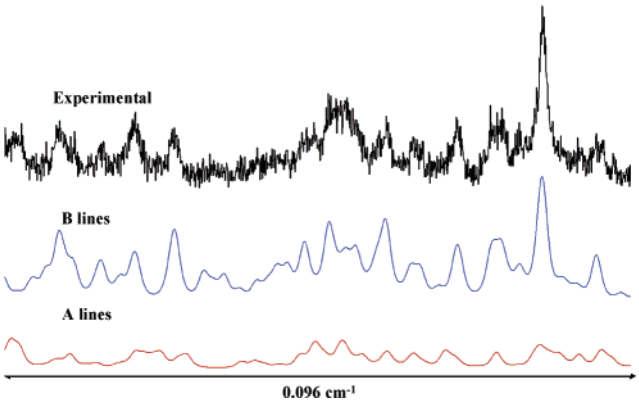

Figure 3. Portion of the high-resolution spectrum of *p*DFB−H_2O at full experimental resolution, extracted from the R branch of the stronger subband. The top trace is the experimental spectrum. The second and third traces show the separate calculated contributions of the two subbands in this region.

TABLE 1: Inertial Parameters of PDFB and Its Water Complex in the Zero-Point Vibrational Levels of Their S_0 and S_1 Electronic States

			*p*DFB−H_2O	
	parameter	*p*DFB[a]	A subband	B subband
S_0	A, MHz	5637.6 (2)	3310.0 (2)	3309.6 (2)
	B, MHz	1428.0 (1)	806.1 (1)	806.1 (1)
	C, MHz	1139.4 (1)	648.7 (1)	648.8 (1)
	ΔI, amu Å	−0.00 (5)	−0.68 (15)	−0.68 (15)
S_1	A, MHz	5283.2 (2)	3185.1 (2)	3184.6 (2)
	B, MHz	1434.2 (1)	795.4 (1)	795.5 (1)
	C, MHz	1128.5 (1)	637.1 (1)	637.1 (1)
	ΔI, amu Å	−0.20 (5)	−0.80 (15)	−0.74 (15)

[a] Reference 28.

$\Delta I' = -0.74$ amu Å^2 in the excited state), but significantly larger than those of bare molecule ($\Delta I'' = 0.00(5)$ amu Å^2, $\Delta I' = -0.20(5)$ amu Å^2).[28] However, the values for *p*DFB−water are still smaller than those expected for two out-of-plane hydroxy hydrogen atoms. While it is difficult to reach structural conclusions based on the results for a single isotopomer, the data suggest that, on average, the oxygen atom and one hydrogen atom of the water molecule lie in the plane and that the second hydrogen atom lies out of the plane. Both hydrogens undergo large amplitude motion along out-of-plane coordinates. For comparison, the indole−water complex[12] exhibits an inertial defect of $\Delta I'' = -1.41$ amu Å^2 in the ground state. This is about twice *p*DFB−water's value. The differences are mainly explained by out-of-plane vibrational motions of the two hydrogens in water. Indole itself is essentially planar in both electronic states, and both water hydrogens are out-of-plane in the complex. Therefore, we suggest that the inertial defect of about −0.7 amu Å^2 in *p*DFB−water can be explained if, on average, one of the two water hydrogens is displaced out-of-plane.

More information about the structure of the complex and the possible motions of water can be deduced from the Kraitchman analysis[30] shown in Table 2. This analysis gives the position of the center-of-mass (COM) of the attached molecule from a comparison of the moments of inertia of the bare molecule and the complex. The relatively small, nonzero $|c|$ values in both electronic states are due to the out-of-plane motions of the two hydroxy hydrogen atoms. The in-plane displacements $|a| = 3.605$ and $|b| = 2.85$ Å in the ground state increase on electronic excitation by 0.05−0.10 Å. An increase in these distances is consistent with decreasing the strength of the hydrogen-bonding

TABLE 2: Center of Mass (COM) Coordinates of the Water Molecule in the Principal Axis Frames of the Bare *p*DFB Molecule and of the *p*DFB−H_2O Complex

state	coordinate	*p*DFB frame (Å)	complex frame (Å)
S_0	$\|a\|$	3.605(5)	3.848(7)
	$\|b\|$	2.858(4)	1.132(3)
	$\|c\|$	0.23(3)	0.067(9)
	$\|r\|$	4.6545(5)	4.012(6)
S_1	$\|a\|$	3.703(5)	3.916(8)
	$\|b\|$	2.905(3)	1.107(2)
	$\|c\|$	0.24(3)	0.065(10)
	$\|r\|$	4.713(5)	4.070(6)

interactions, which is responsible for the blue shift of the origin band of the water complex relative to that of the bare molecule.

It is interesting to compare the results for *p*DFB−water to those for the analogous benzonitrile−water (BN−water) complex.[31−34] In both complexes, the oxygen is bound to an ortho hydrogen and one hydroxy hydrogen is bound to the fluorine or the cyano group. In the electronic ground-state S_0, the structures of these complexes are very similar. The water COM in BN−water is slightly further away from the aromatic ring (coordinates with respect to the ring center: 3.59/3.14/0.00 Å). However, *p*DFB−water and BN−water differ in their behavior upon excitation into S_1. Whereas there is no significant change in the *a* and *b* COM coordinates in BN−water (they decrease by less than 0.01 Å), the coordinates increase by 0.05−0.10 Å in *p*DFB−water. The larger structural change in *p*DFB−water also is reflected in the larger blue shift of the origin of the complex with respect to that of the monomer: 168.1 cm^{-1} in *p*DFB. In contrast, BN−water exhibits a red shift of −69.8 cm^{-1} with respect to that of BN itself.[34]

Nuclear Spin Statistical Weights. Because of the D_{2h} symmetry of *p*DFB and the C_{2v} symmetry of H_2O, the molecular symmetry (MS) group[35] of the complex is G_{16}. Assuming that only the two hydrogens of H_2O or the *a* inertial axis of *p*DFB are feasible tunneling paths connecting symmetrically equivalent configurations, the effective molecular symmetry group is G_8 which is isomorphic with D_{2h} (see Table 3). Exchanging the two hydrogens of H_2O corresponds to the permutation $P_1 = (ab)$, and rotating around the *a* inertial axis of *p*DFB corresponds to $P_2 = (26)(35)$. The full molecular symmetry group G_{16} can be obtained by $G_{16} = G_8 \otimes \{E, (14)(23)(56)\}$, where the permutation (14)(23)(56) corresponds to an internal rotation around the *b* inertial axis of *p*DFB.

In Table 3, classifications of the rovibronic wave functions according to the symmetry species of the molecular symmetry group G_8 are given (in G_{16}, add the superscript + to the symmetry labels of Γ_{el} and Γ_{rot}). According to the general selection rule for electric dipole transitions ($\Gamma_{rve}' \otimes \Gamma_{rve}'' \supset \Gamma_2^{+(+)}$), electronic transitions within one tunneling state follow μ_b-type selection rules whereas μ_a-type transitions are possible between the different substates of a *p*DFB internal rotation around its *a* axis. Therefore, μ_a- type transitions are theoretically split, but the splitting is expected to be too small to be observed in the UV spectrum.

Nuclear spin statistical weights can be used to determine which nuclei are involved in the large amplitude motion producing the observed splitting. These weights are determined by the fact that rovibronic states having symmetry Γ_{rve} can only combine with a nuclear state having symmetry Γ_{nspin} in the molecular symmetry group if the product of these symmetries $\Gamma_{rve} \otimes \Gamma_{nspin}$ contains Γ_{int}.[35] Γ_{int} is the complete internal wave function and must be antisymmetric with respect to any odd permutation of fermions. Therefore, Γ_{int} is $\Gamma_3^{+(-)}$ or $\Gamma_4^{+(-)}$ as

TABLE 3: Character Table of the Molecular Symmetry Group G_8 of *p*-Difluorobenzene−Water and Symmetry Species of the Rotational and Electronic States[a]

	E $(R^0)^b$	P_1 $(R^0)^b$	E* $(R_y^\pi)^b$	P_1* $(R_y^\pi)^b$	P_2 $(R_z^\pi)^b$	P_2P_1 $(R_z^\pi)^b$	P_2^* $(R_x^\pi)^b$	$P_2P_1^*$ $(R_x^\pi)^b$	w^+,w^{-c}	ψ_{rot} (K_aK_c)	ψ_e
Γ_1^+	1	1	1	1	1	1	1	1	16, 24	ee	S_0
Γ_2^+	1	1	−1	−1	1	1	−1	−1	16, 24	eo	
Γ_3^+	1	−1	1	−1	1	−1	1	−1	48, 72		
Γ_4^+	1	−1	−1	1	1	−1	−1	1	48, 72		
Γ_1^-	1	1	1	1	−1	−1	−1	−1	12, 12	oe	S_1
Γ_2^-	1	1	−1	−1	−1	−1	1	1	12, 12	oo	
Γ_3^-	1	−1	1	−1	−1	1	−1	1	36, 36		
Γ_4^-	1	−1	−1	1	−1	1	1	−1	36, 36		

[a] $P_1 = (ab)$ is the permutation of the water hydrogen nuclei, $P_2 = (26)(35)$ is the permutation of the *p*DFB nuclei symmetric to its *a* axis. The molecule fixed axis system (x,y,z) is defined so that the carbon or fluorine nucleus labeled 1 of *p*DFB has a positive *z* coordinate and the carbon or hydrogen labeled 2 a positive *x* coordinate. [b] Equivalent rotations. [c] Nuclear spin statistical weight (the superscripts refer to G_{16}; weights for G_8: $w = w^+ + w^-$).

the parity is + or − (see Table 3). (The second superscript in parentheses describes the classification in G_{16} and can be dropped in G_8.) In G_8, the proton spin functions of *p*DFB generate the representation $\Gamma_{nspin}^{H} = 10\,\Gamma_1^+ \oplus 6\Gamma_1^-$, whereas in G_{16} the hydrogen and fluorine nuclei have to be considered, generating the representation $\Gamma_{nspin}^{F,H} = 24\,\Gamma_1^{+(+)} \oplus 16\,\Gamma_1^{+-} \oplus 12\Gamma_1^{-+} \oplus 12\Gamma_1^{--}$. The H_2O hydrogen nuclei generate the representation $\Gamma_{nspin}^{H} = 3\,\Gamma_1^{+(+)} \oplus \Gamma_3^{+(+)}$. The derived nuclear spin statistical weights *w* are given in Table 3. It can be easily seen that only a large amplitude motion which interchanges the water hydrogens leads to the observed 1:3 intensity ratio between the two subbands A and B in the UV spectrum. An internal rotation of *p*DFB around its *a* inertial axis would give a 10:6 ratio and a rotation around its *b* or *c* axes would give a 7:9 ratio. Other factors could contribute to the observed ratios, but these factors are expected to be small at the vibrational temperatures typically achieved in our apparatus.

Analysis of Internal Motion. More specific information about the motion of the water molecule in the complex comes from an analysis of the observed tunneling splitting of 3.63 GHz and the relatively small but significant differences in the rotational constants of the two subbands in both electronic states (cf. Table 1). The 3.63 GHz splitting of the two subbands is equal to the difference in the subtorsional splittings in the two electronic states because the observed transitions obey the selection rule $\Delta\sigma = 0$. The two subbands have different intensities since $\sigma = 0$ and 1 levels have different nuclear spin statistical weights. Also, each of the subbands has different rotational constants because of the coupling between torsional motion of water and overall rotation. The differences between the rotational constants of two subbands are calculated from $\Delta A'' = A_{v0}'' - A_{v1}''$, $\Delta A' = A_{v0}' - A_{v1}'$ and so forth.[36] According to Table 1, the rotational constants of the two subbands of the water complex are the same to within the error limits except for the *A* values; $\Delta A'' = 0.4$ MHz in the ground state and $\Delta A' = 0.5$ MHz in the excited state. This shows that the axis about which the motion of the water molecule is primarily occurring in the two states is approximately the same and further that this axis is approximately parallel to the *a* principal inertial axis of the complex.

As discussed in the analysis of the tunneling splitting in BN−water,[34] there exist several possible models for the motion of the attached water molecule. All require the breaking and remaking of at least one of the hydrogen bonds (F---H−O or H---O−H). One of the simplest models is an internal rotation of the H_2O about its C_2-(*b*-)axis within a planar equilibrium structure. The spectrum was analyzed with a semirigid internal rotor model consisting of a rigid frame with C_s symmetry and one rigid internal rotor of C_{2v} symmetry.[37,38] For each electronic state, the molecule-fixed axis system (*x*, *y*, *z*) was rigidly attached to the frame with its origin at the COM of the whole molecule. The *z* axis was chosen to be parallel to the internal rotation axis, and the *y* axis was chosen to be parallel to the complex *c* principal axis, perpendicular to the symmetry plane of the frame. In a least-squares fit, the moments of inertia of the complex I_{xx}, I_{yy}, I_{zz}, and the potential term V_2 of the potential $V(\tau) = V_2(1 - \cos 2\tau)/2$ for both states were determined. The planar moment of the H_2O internal rotor P_x was fixed to the value obtained from ground-state rotational constant $B_0 = 435$ GHz.[39] This procedure yields upper limits for the V_2 potential barriers of $V_2'' = 450$ cm^{-1} and $V_2' = 290$ cm^{-1}. The angle θ between the internal rotation axis and the *a* principal axis of the complex was estimated to be about 70° in S_1 whereas no preferred orientation was found for S_0. This result leads to a predicted subband splitting of 3.6 GHz, in good agreement with the experimental value of 3.63 GHz. However, it is clear that the axis about which the water molecule is moving in the ground state cannot be its *b* axis. Such a motion would require a breaking of the hydrogen bond, a much higher energy process than 450 cm^{-1}. With the value $\theta = 70°$ in the excited state, since the internal rotation axis also has a component along the *b* axis, the rotational B constant of the complex also should be perturbed. However, no difference in the *B* values of the two subbands was observed.

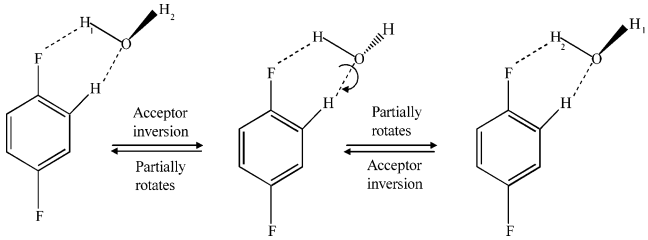

Figure 4. Combined inversion and restricted internal rotation of the water molecule in *p*DFB−H_2O.

In a second model, the water molecule was assumed to rotate about an axis in its *bc* plane, 55° off its *b* axis ($F = 339$ GHz[39]), which corresponds to a rotation about one of the lone pairs of the oxygen atom. This motion[40] leads to a barrier estimate of $V_2'' = 330 \pm 20$ cm^{-1} in the ground state and $V_2' = 230 \pm 30$ cm^{-1} in the excited state, with a predicted subband splitting of 3.33 ± 0.9 GHz, in good agreement with the experimental value of 3.63 GHz. However, this simple motion does not provide for the equivalent exchange of the two hydrogens, which is needed to reproduce the observed 1:3 intensity ratio.

In the third, and preferred model, the observed tunneling splitting and differences in rotational constants are attributed to the combined effects of inversion and restricted internal rotation, as shown in Figure 4. While this process may be visualized as consisting of two separate steps, switching of the

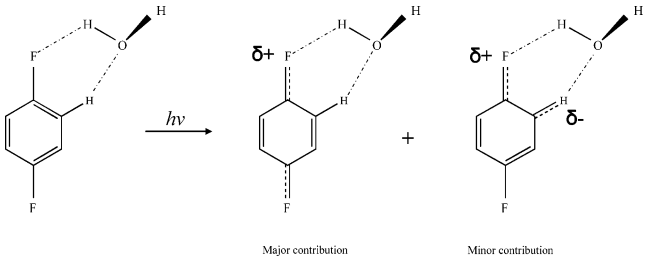

Figure 5. Light-induced changes in the electron distribution of *p*DFB are responsible for the differences in the intermolecular potentials of *p*DFB−H_2O in its ground and electronically excited states.

lone pairs and restricted internal rotation of the water molecule, the net effect is a C_2 rotation of the water about its *b* symmetry axis. The two motions taken together are equivalent to the acceptor-switching motion in the H_2O dimer.[41] Importantly, the combined motion renders the two hydroxyl hydrogens equivalent, explaining the observed 1:3 intensity ratio.

In this model, the determined values of V_2 ($V_2'' = 330$ and $V_2' = 230$ cm^{-1}) are the effective barrier heights for the combined inversion-torsional motion. However, we imagine that the two steps make different contributions to V_2. The barrier to water inversion in ground-state *p*DFB−water is likely to be relatively low, probably much less than the 130 cm^{-1} barrier in the water dimer.[41] In contrast, the barrier to the torsional motion of the attached H_2O in *p*DFB−water is likely to be higher, owing to the stronger C−F---H−O interaction. The strength of this interaction is significantly decreased in the S_1 state; a principal reason for this decrease is the electron density redistribution shown in Figure 5. As we have seen, the fluorine lone pair electron density in the S_1 state of *p*DFB−water is significantly reduced, compared to the ground state, leading to a significantly reduced value of V_2 in the excited state. MP2/6-31G** calculations confirm that, in the ground state, the C−F---H−O binding energy is about 300 cm^{-1}, whereas the C−H--O−H binding energy is much weaker, 30 cm^{-1} or so.

The geometry of the C−F---H−O intermolecular interaction is considerably different from those of O−H---O and O−H---N hydrogen bonds. Whereas the normal hydrogen-bonding angle is almost linear, the angle C−F---H in *p*DFB−water is significantly decreased to around 110°,[22] making for weaker interactions. In comparison with CH_2F_2−water (∼700 cm^{-1}),[23] our O−H---F intermolecular interaction (∼300 cm^{-1}, including the water inversion motion) appears to be significantly weaker. Arguably, the acceptor ability of C(sp^2)−F is not as good as that of C(sp^3)−F. Still, the strength of any hydrogen bond depends more on donor acidity than on acceptor basicity, an effect that is nicely confirmed by comparisons of the properties of *p*DFB and BN water complexes. The V_2 barriers in BN−water are nearly the same in both states.[34] There are obviously only very small changes in the electronic structure of BN upon excitation, which is also indicated by a small increase of its dipole moment (+0.09 D).[42]

Summary

The structural and dynamical properties of a binary complex between *p*-difluorobenzene (*p*DFB) and water are revealed by studies of its high-resolution electronic spectrum in the collision-free region of a molecular beam. The complex exhibits two hydrogen bonds, a stronger F---H−O bond in which the attached water molecule acts as a proton donor and a weaker H---O−H bond in which the attached water molecule acts as a proton acceptor, resulting in a (heavy-atom) planar structure. The water molecule also is observed to move within the complex. The motion is a combined inversion-internal rotation, opposed by a barrier of ∼330 cm^{-1} in the ground electronic state. Reduction of this barrier to ∼230 cm^{-1} in the electronically excited state is attributed to light-induced changes in the π-electron distribution in the aromatic ring.

Acknowledgment. We thank John T. Yi for helpful discussions. This work was supported by NSF (CHE-0315584).

References and Notes

(1) Brutschy, B. *Chem. Rev.* **2000**, *100*, 3891.
(2) Kim, K. S.; Tarakeshwar, P.; Lee, J. Y. *Chem. Rev.* **2000**, *100*, 4145.
(3) Gerhards, M.; Schmitt, M.; Kleinermanns, K.; Stahl, W. *J. Chem. Phys.* **1996**, *104*, 967.
(4) Berden, G.; Meerts, W. L.; Schmitt, M.; Kleinermanns, K. *J. Chem. Phys.* **1996**, *104*, 972.
(5) Melandri, S.; Maris, A.; Favero, P. G.; Caminati, W. *Chem. Phys.* **2002**, *283*, 185.
(6) Barth, H.-D.; Buchhold, K.; Djafari, S.; Reimann, B.; Lommatzsch, U.; Brutschy, B. *Chem. Phys.* **1998**, *239*, 49.
(7) Becucci, M.; Pietraperzia, G.; Pasquini, M.; Piani, G.; Zoppi, A.; Chelli, R.; Castellucci E.; Demtröder, W. *J. Chem. Phys.* **2004**, *120*, 5601.
(8) Ribblett, J. W.; Sinclair, W. E.; Borst, D. R.; Yi, J. T.; Pratt, D. W. submitted.
(9) Spoerel, U.; Stahl, W. *J. Mol. Spectrosc.* **1998**, *190*, 278.
(10) Tubergen, M. J.; Andrews, A. M.; Kuczkowski, R. L. *J. Phys. Chem.* **1993**, *97*, 7451.
(11) Carney, J. R.; Hagemeister, F. C.; Zwier, T. S. *J. Chem. Phys.* **1998**, *108*, 3379.
(12) Korter, T. M.; Pratt, D. W.; Küpper, J. *J. Phys. Chem. A* **1998**, *102*, 7211.
(13) Gotch, A. J.; Zwier, T. S. *J. Chem. Phys.* **1992**, *96*, 3388.
(14) Suzuki, S.; Green, P. G.; Bumgarner, R. E.; Dasgupta, S.; Goddard, W. A., III; Blake, G. A. *Science* **1992**, *257*, 942.
(15) Gutowsky, H. S.; Emilsson, T.; Arunan, E. *J. Chem. Phys.* **1993**, *99*, 4883.
(16) Pribble, R. N.; Garrett, A. W.; Haber, K.; Zwier, T. S. *J. Chem. Phys.* **1995**, *103*, 531.
(17) Emilsson, T.; Gutowsky, H. S.; de Oliveira, G.; Dykstra, C. E. *J. Chem. Phys.* **2000**, *112*, 1287.
(18) Garrett, A. W.; Zwier, T. S. *J. Chem. Phys.* **1992**, *96*, 3402.
(19) Pribble, R. N.; Zwier, T. S. *Faraday Discuss. Chem. Soc.* **1994**, *97*, 229.
(20) Solcà, N.; Dopfer, O. *Chem. Phys. Lett.* **2001**, *347*, 59.
(21) Brenner, V.; Martrenchard-Barra, S.; Millie, P.; Dedonder-Lardeux, C.; Jouvet, C.; Solgadi, D. *J. Phys. Chem.* **1995**, *99*, 5848.
(22) Tarakeshwar, P.; Kim, K. S.; Brutschy, B. *J. Chem. Phys.* **1999**, *110*, 8501.
(23) Caminati, W.; Melandri, S.; Rossi, I.; Favero, P. G. *J. Am. Chem. Soc.* **1999**, *121*, 10098.
(24) Smith, B. J.; Swanton, D. J.; Pople, J. A.; Schaefer, H. F., III; Radom, L. *J. Chem. Phys.* **1990**, *92*, 1240.
(25) Thalladi, V. R.; Weiss, H. C.; Blaser, D.; Boese, R.; Nangia, A.; Desiraju, G. R. *J. Am. Chem. Soc.* **1998**, *120*, 8702.
(26) Majewski, W. A.; Pfanstiel, J. F.; Plusquellic, D. F.; Pratt, D. W. In *Laser Techniques in Chemistry*; Myers A. B., Rizzo, T., Eds.; Wiley: New York, 1995; pp 101−148.
(27) Gerstenkorn, S.; Luc, P. *Atlas du spectre d'absorption de la molecule d'iode*; CNRS: Paris, 1978.
(28) Sussman, R.; Neuhauser, R.; Neusser, H. J. *Can. J. Phys.* **1994**, *72*, 1179. See also Schäfer, M.; Kang, C. H.; Pratt, D. W. *J. Phys. Chem. A* **2003**, *107*, 10753.
(29) Described in Plusquellic, D. F.; Suenram, R. D.; Maté, B.; Jensen, J. O.; Samuels, A. C. *J. Chem. Phys.* **2001**, *115*, 3057.
(30) Kraitchman, J. *Am. J. Phys.* **1953**, *21*, 17.
(31) Helm, R. M.; Vogel, H.; Neusser, H. J.; Storm, V.; Consalvo, D.; Dreizler, H. *Z. Naturforsch. Teil A* **1997**, *52*, 655.
(32) Storm, V.; Dreizler, H.; Consalvo, D. *Chem. Phys.* **1998**, *239*, 109.
(33) Melandri, S.; Consalvo, D.; Caminati, W.; Favero, P. G. *J. Chem. Phys.* **1999**, *111*, 3874.
(34) Schäfer, M.; Borst, D. R.; Pratt, D. W.; Brendel, K. *Mol. Phys.* **2002**, *100*, 3553.
(35) Bunker, P. R. *Molecular Symmetry and Spectroscopy;* Academic Press: New York/San Francisco/London, 1979.
(36) Tan, X. Q.; Majewski, W. A.; Plusquellic, D. F.; Pratt, D. W. *J. Chem. Phys.* **1991**, *94*, 7721.
(37) Bauder, A.; Mathier, E.; Meyer, R.; Ribeaud, M.; Günthard, H. H. *Mol. Phys.* **1968**, *15*, 597.

(38) Schäfer, M. *J. Chem. Phys.* **2001**, *115*, 11139.
(39) DeLucia, F. C.; Helminger, P.; Cook, R. L.; Gordy, W. *Phys. Rev.* **1972**, *A5*, 487.
(40) Actually, because of electron repulsion between the lone pairs of the fluorine and oxygen atoms, the water molecule does not freely rotate about the axis of the H---O−H hydrogen bond. The two hydroxyl hydrogens experience a simultaneous inversion in the course of its internal rotation motion.
(41) Fellers, R. S.; Braly, L. B.; Saykally, R. J.; Leforestier, C. *J. Chem. Phys.* **1999**, *110*, 6306, and references therein.
(42) Borst, D. R.; Korter, T. M.; Pratt, D. W. *Chem. Phys. Lett.* **2001**, *350*, 485.